Application of high silica zeolite ZSM-5 in a hybrid treatment process based on sequential adsorption and ozonation for VOCs elimination

Hicham Zaitan, Marie-Hélène Manero, Héctor Valdés

Application of high silica zeolite ZSM-5 in a hybrid treatment process based on sequential adsorption and ozonation for VOCs elimination

Hicham Zaitan[1,*], *Marie Hélène Manero*[2,3], *Héctor Valdés*[4]

1. *Laboratoire de Chimie de la Matière Condensée (LCMC), Faculté des Sciences et Techniques, Université Sidi Mohamed Ben Abdellah, B.P. 2202, Fès , Maroc*
2. *Université de Toulouse, INPT, UPS, Laboratoire de Génie Chimique, 4, Allée Emile Monso, F-31030 Toulouse, France*
3. *CNRS, Laboratoire de Génie Chimique, F-31030 Toulouse, France*
4. *Laboratorio de Tecnologías Limpias (F. Ingeniería), Universidad Católica de la Santísima Concepción, Alonso de Ribera 2850, Concepción, Chile*

A B S T R A C T

In this study, a hydrophobic synthetic zeolite, namely ZSM-5 is chosen as an adsorbent/catalyst for toluene removal. Experimental results showed that toluene adsorption onto ZSM-5 was favourable, following a Langmuir adsorption isotherm model. ZSM-5 zeolite was regenerated using gaseous ozone at low temperature. Adsorbed toluene was oxidised, releasing mainly CO_2 and H_2O. Traces of oxidation by-products such as acetic acid and acetaldehyde were formed and remained adsorbed after the oxidative regeneration with ozone. After four successive cycles of adsorption/ozonation, the adsorption efficiency was not affected (92%–99%). These results showed that volatile organic compound (VOC) removal by adsorption onto ZSM-5 zeolite followed by ozone regeneration could be used as a promising hybrid process for the control of VOC emissions in terms of efficiency.

Keywords:
Adsorption
Ozone
Toluene
VOCs
Zeolite

Introduction

Volatile organic compounds (VOCs) are often considered as toxic chemicals that cause severe health problems. Their elimination has been a serious challenge for several years for many industrial companies which have to accomplish stringent environmental regulations (Ruddy and Carroll, 1993; VOC Solvents Directive, 1999/13/EC, 1999; Paints Directive, 2004/42/EC, 2004). Conventional methods used to treat VOCs include absorption, thermal and catalytic oxidations, biofiltration, condensation and adsorption (Ruddy and Carroll, 1993; Khan and Ghoshal, 2000; Brosillon et al., 2001; Ghoshal and Manjare, 2002; Yang et al., 2013; Li et al., 2014). Among them, adsorption has been considered as one of the best options to treat VOC emissions (Foster et al., 1992; Zaitan et al., 2013; Le Cloirec, 1998; Brosillon et al., 2001). However, adsorption techniques only transfer pollutants from one phase to another one, generating a new waste with a higher content of VOCs.

Regarding this problem, a variety of regeneration techniques have been evaluated and implemented. Regeneration is normally performed by changing the conditions in the adsorber bed in order to desorb the VOCs from the adsorbent (Yang, 1987; Le Cloirec, 1998; Bonjour et al., 2002; Yu et al., 2007). This process is achieved either by increasing the temperature using hot air or

* *Corresponding author*. E-mail: hicham.zaitan@usmba.ac.ma (Hicham Zaitan).

http://dx.doi.org/10.1016/j.jes.2015.05.021

steam, by decreasing the partial pressure, or by introducing a stronger adsorbate able to displace the adsorbed VOCs (Rafson, 1998). However, the regeneration of adsorbents such as activated carbons is very difficult because of their thermal and chemical instabilities that may cause significant safety problems (Blocki, 1993; Baek et al., 2004).

Recently, the use of hydrophobic zeolites has been attracting more and more attention because of their non-flammability, thermal stability and resistance to humidity (Brosillon et al., 2001; Vinh-Thang et al., 2005; Cosseron et al., 2013). The application of hydrophobic zeolites as a dual function adsorbent/catalyst medium is justified in two aspects. Firstly, hydrophobic zeolites are safe to use in catalytic oxidation processes operating at high temperatures. Secondly, they have a high adsorption affinity toward VOC under humid conditions (Bonjour et al., 2002).

In the last years, the combined use of adsorption followed by ozone oxidation (denoted as AD-OZ process) at laboratory and at bench scale has been investigated and may offer an interesting potential for its implementation at industrial scale, since ozone can destroy adsorbed molecules, regenerating the zeolite adsorption capacity (Monneyron et al., 2007; Brodu et al., 2012). However, very few studies are focused on coupling ozone and synthetic zeolites in a same process treatment to remove VOCs (Monneyron et al., 2003, 2007; Kwong et al., 2008; Einaga et al., 2011; Brodu et al., 2012).

The adsorption of VOCs on several kinds of zeolites followed by ozonation resulted in a high degree of recovery on the adsorption capacity of zeolites (Monneyron et al., 2003, 2007). In this hybrid treatment, it has been claimed that molecular ozone generates very powerful free radicals after ozone adsorption and its decomposition on strong Lewis acid sites of zeolite surface, leading to the oxidation of adsorbed VOCs (Brodu et al., 2013; Alejandro et al., 2014).

This work aims to investigate the main operating process parameters that influence the efficiency of a new hybrid process of VOC adsorption onto a fixed-bed of ZSM-5 followed by gaseous ozone oxidation in a single reactor. In particular, the maximum adsorption capacity of zeolite and the degree of adsorption capacity recovery after various cycles of adsorption–ozonation were assessed at bench scale. Moreover, oxidation by-products was identified and mass balances were established. As a result, process efficiency was evaluated in order to process design and optimisation.

1. Materials and methods

1.1. Materials

A commercial high silica zeolite (ZSM-5) was used in the adsorption–ozonation process (AD–OZ) and was supplied by (TOSOH Corporation, Tokyo, Japan) in the form of pellets (Ø = 1.5 mm). Zeolite was dried in air at 500 K for 24 hr and stored in a dessicator for further use. Table 1 shows the key physical–chemical properties of ZSM-5 zeolite.

Ozone was generated from dry air using an ozone generator (Trailigaz Model 5LO, Trailigaz Ozone S.A.S., Saint Maurice, France) featuring a variable ozone production rate, with a maximum of around 24 g O_3/hr. Gaseous ozone stream was humidified (60% of relative humidity) by bubbling the outlet stream of ozone coming from the ozone generator into a water column. Toluene (purity > 99%) was supplied in liquid phase by Sigma-Aldrich (Sigma-Aldrich Chimie S.a.r.l., Lyon, France) and was used in this study as a target organic molecule representative of VOCs.

Table 1 – Physical–chemical properties of ZSM-5 zeolite.

Property	Value
Crystalline framework	Interconnected channels
Pore diameters (Å)	Intersections: 6 × 8 Channels: 5.1 × 5.5 and 5.3 × 5.6
SiO_2/Al_2O_3 (mol/mol)	2100
Total pore volume V_T (cm^3/g)	0.18
Micropore volume V_{micro} (cm^3/g)	0.11
Mesopore volume V_{meso} (cm^3/g)	0.07
Specific surface area S_{BET} (m^2/g)	308
Granular diameter (mm)	1.5
Clay binder content (%)	20
Concentration of Lewis acid sites (μmol/g)	28 (Brodu et al., 2013)
Concentration of Brønsted acid sites (μmol/g)	4 (Brodu et al., 2013)
Compensating cation	H

1.2. Adsorption isotherms

Toluene adsorption isotherms were performed using the bottle point method, as described elsewhere (Brosillon et al., 2001). Different amounts of zeolite mass (ranging from 0.3 to 1 g) were introduced into batch glass contactors (1.1 dm^3). Then, a fixed volume of liquid toluene (typically 50 μL) was injected through a septum into each adsorption chamber at 300 K and 101 kPa, leading to an initial concentration of about 0.5 mol/m^3 after the complete evaporation of toluene. After that, adsorption chambers were stirred until the equilibrium was reached (2 hr). Finally, gas samples were taken from each bottle and analysed by gas chromatography (Varian CP-3800 GC, Varian Inc., Walnut Creek, USA). The total amount of adsorbed toluene per gramme of zeolite at the equilibrium, q_e (mol/kg), was calculated from a mass balance in each isotherm batch adsorption chamber, as follows:

$$q_e = \frac{(C_0 - C_e)V}{M} \quad (1)$$

where C_0 and C_e (mol/m^3) are gas phase concentration of toluene at initial and at equilibrium, respectively, M (g) is the mass of zeolite sample used in each batch adsorption chamber, and V (1.1×10^{-3} m^3) stands for the total volume of the adsorption chamber. Adsorbed quantities were normalised for pure zeolite material, supposing that inert clay binder mass did not participate in the adsorption phenomena.

1.3. Experimental procedures of the adsorption–ozonation process

Experimental set-up presented in Fig. 1 consists of four main parts: a toluene vapour saturator, a fixed-bed glass contactor (80 mm ID, 200 mm length), gas analysers, and an exhaust gas trap.

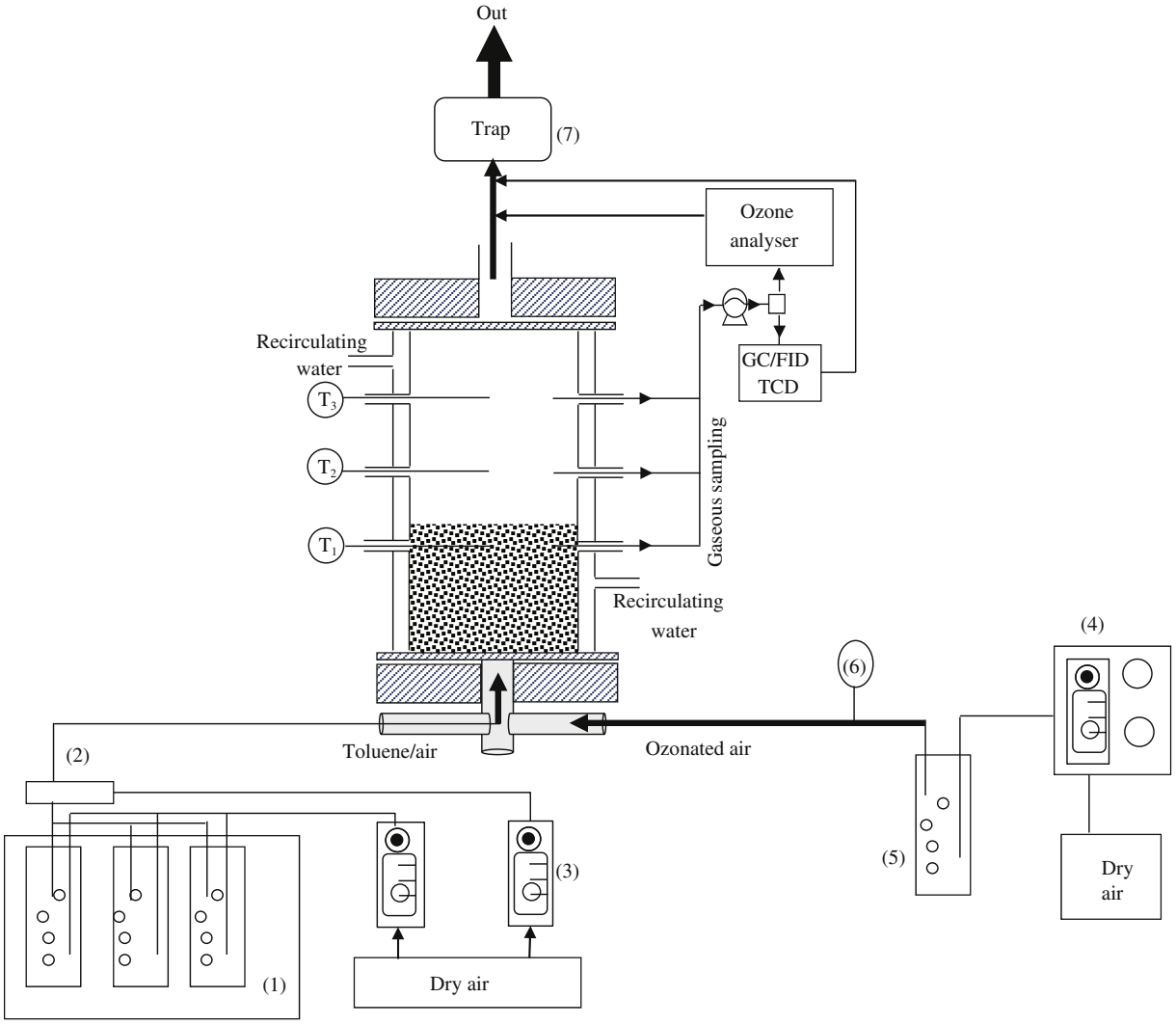

Fig. 1 – Experimental set-up of the adsorption (AD)–ozonation (OZ) system: (1) toluene saturator chamber, (2) mixer, (3) mass flow controllers, (4) ozone generator, (5) humidifier, (6) humid sensor, and (7) exhaust gas trap. GC: gas chromatography; FID: flame ionisation detector; TCD: thermal conductivity detector.

The inlet concentration of toluene (C_{in}) was fixed by bubbling dry air into pure liquid toluene, using a temperature controlled bath (300 K), and diluted to a desired concentration by mixing with a fresh dry air stream. Sequential adsorption–ozonation experiments were carried out in the fixed-bed glass contactor loaded with 150 g of the zeolite sample. Both adsorption and ozonation steps were conducted under dynamic conditions at room temperature (300 K) and atmospheric pressure. A total flow rate of 5 m^3/hr (residence time < 0.2 sec) containing 50 ppmV (0.205 g/m^3) of toluene was continuously supplied over the zeolite bed. The adsorption step was completed when the outlet concentration of toluene reached 35% of the inlet concentration ($C_{out}/C_{in} \approx 0.35$). After that, a regeneration step was performed using a humidified gaseous ozone stream (25 dm^3/hr, 18 g_{O3}/m^3, and 60% of relative humidity). During the regeneration step, the outlet concentration of O_3, toluene and its oxidation by-products was continuously analysed. Data were recorded every 13 min. Ozone regeneration was stopped when CO_2 was no longer detected at the reactor outlet stream and the reactor temperature returned to room temperature (300 K), indicating the end of the oxidation reactions. The exhaust gas stream was sent to a trap before discharging to the ambient air.

The total amount of adsorbed toluene per mass of zeolite ($Q^A_{C_7H_8}$, $g_{C_7H8}/g_{ZSM\text{-}5}$) during the adsorption step was calculated according to Eq. (2):

$$Q^A_{C_7H_8} = \frac{F\,C_{in}}{m}\int_0^{t_A}\left(1-\frac{C_{out_t}}{C_{in}}\right)dt \qquad (2)$$

where F (m^3/min) is the gas flow rate, m (g) is the mass of ZSM-5 zeolite, C_{in} (g/m^3) is the inlet concentration of toluene, t_A (min) is the adsorption time to reach saturation, and C_{out_t} (g/m^3) is the outlet concentration of toluene as a function of time.

The total applied load of ozone per mass of zeolite ($Q^L_{O_3}$, gO_3/gZSM-5) during the ozonation step was calculated using

the following equation:

$$Q^{L}_{O_3} = \frac{F\ C_{O_{3in}}}{m} \int_{t_A}^{t_B} dt \tag{3}$$

where $C_{O_{3in}}$ (g/m^3) is the inlet concentration of ozone, and t_A and t_B (min) correspond to the starting and ending time of the ozonation step, respectively.

The total amount of desorbed toluene per mass of zeolite ($Q^{D}_{C_7H_8}$, $g_{C_7H8}/g_{ZSM\text{-}5}$) due to local heating generated during the ozonation step was obtained using Eq. (4):

$$Q^{D}_{C_7H_8} = \frac{F}{m} \int_{t_A}^{t_B} C_{out_t} dt. \tag{4}$$

The total amount of carbon dioxide formation per mass of zeolite (Q_{CO_2} , $g_{CO_2}/g_{ZSM\text{-}5}$) during the ozonation step was calculated applying Eq. (5):

$$Q_{CO_2} = \frac{F}{m} \int_{t_A}^{t_B} C_{CO_{2_t}} dt \tag{5}$$

where $C_{CO_{2_t}}$ (g/m^3) represents the outlet concentration of carbon dioxide as a function of time.

1.4. Analytical methods

Toluene and CO_2 concentrations at the reactor outlet stream were monitored at constant intervals of time with an automatic 10-port injection valve and a digital timer by gas chromatography (Varian CP-3800 GC, Varian Inc., Walnut Creek, USA). Toluene and its oxidation by-products of high molecular weight were analysed using a CP-SIL 8 capillary column (30 m length × 0.53 mm ID) with a 1.0 μm film thickness coupled to a flame ionisation detector (FID); whereas CO_2 was analysed with a HayeSep Q packed-bed column (80–100 mesh particle size, 0.91 m length × 3.18 mm OD), using a thermal conductivity detector (TCD). Data were recorded every 5 min and processed with a Galaxie Chromatography Data System (Galaxie CDS Software, Varian Inc., Walnut Creek, USA). Ozone concentration was registered on-line, using an ozone analyser (BMT 963 Model, BMT MESSTECHNIK GMBH, Berlin, Germany).

2. Results and discussion

2.1. Adsorption equilibrium isotherms of toluene

Experimental adsorption isotherms were fitted to Langmuir (Langmuir, 1916), Freundlich (Freundlich, 1906) and Toth (Toth, 1971) equations, which have been intensively used to describe adsorption isotherms on zeolites (Einaga et al., 2011). The models express the adsorbed quantity of toluene per mass of zeolite, q_e (mol/kg), as a function of toluene concentration at the equilibrium, C_e (mol/m^3), as follows:

Langmuir equation:

$$q_e = \frac{q_m b\, C_e}{1 + b\, C_e} \tag{6}$$

where q_m (mol/kg) is the maximum adsorption capacity and b (m^3/mol) is the adsorption equilibrium constant or Langmuir coefficient.

Freundlich equation:

$$q_e = k\, C_e^{1/n} \tag{7}$$

where k (mol$^{1-1/n}$·m$^{3-1/n}$/kg) stands for the adsorption equilibrium constant and n is the empirical constant of the Freundlich model.

Toth equation:

Toth isotherm is a semi-empirical expression, normally used to describe a monolayer adsorption. Parameters given in this equation are used to characterise surface heterogeneity and interactions of adsorbed molecules. It is a three-parameter model usually written as follows:

$$q_e = \frac{q_m{}' b'\, C_e}{\left[b' + C_e^{t'}\right]^{1/t'}} \tag{8}$$

where $q_m{}'$ (mol/kg) is the maximum monolayer adsorption capacity parameter, b' ((mol/m^3)$^{t'}$) is the Toth isotherm constant, and t' is a dimensionless constant, usually less than unity. Parameters b' and t' are specifics for the adsorbate–adsorbent systems. The more the parameter t' is away from unity, the more heterogeneous is the system. Parameters q_e, b', and t' in Eq. (8) were determined numerically.

Adsorption equilibrium data of toluene are shown in Fig. 2. As can be observed, at low concentration of toluene a sharp initial increase on the adsorption capacity was observed that could correspond to micropore filling. At a relatively high concentration, a flat plateau region was registered, characteristic of monolayer adsorption on microporous adsorbents. A solid line in Fig. 2 shows that experimental data fit very well the Langmuir adsorption model. Additionally, experimental data were also fitted to other common isotherm models, such as: Freundlich and Toth equations. Although these isotherm equations showed good predictive capabilities; however, they appeared less compatible, with large errors (up to 5%) between the measured and modelled values (Table 2 and Fig. 2).

As can be seen in Fig. 2, the amount of toluene adsorbed on ZSM-5 at 300 K reached a plateau of 0.93 mmol/g. Micropore fillings were calculated using the assumption that the adsorbed phase was comparable to liquid state, highlighting the steric exclusion of toluene on ZSM-5 (58%). This value corresponded to an adsorption of about five toluene molecules per unit of zeolite cell. This result was in agreement with those reported by Meininghaus and Prins (2000) who observed an adsorption capacity of 4.6 molecules per unit cell for HZSM-5/180 and NaZSM-5 (with a framework Si/Al ratio of 180) and 7–7.5 molecules per unit cell for MFI type zeolites reported by Lee and Chaing (1996), Song and Rees (2000), and Song et al. (2007). As a way of comparison, Table 3 lists the amount of adsorbed toluene at the equilibrium on ZSM-5 (obtained in this work) and from literature references, using different adsorbents under similar conditions. As can be seen, the adsorption capacity of ZSM-5 toward toluene was in excellent agreement with the observed values using other porous adsorbents such as NaZSM-5, HMOR (Serra et al., 2012), NaY (Jin and Zhu, 2000), and some activated carbons EA95,

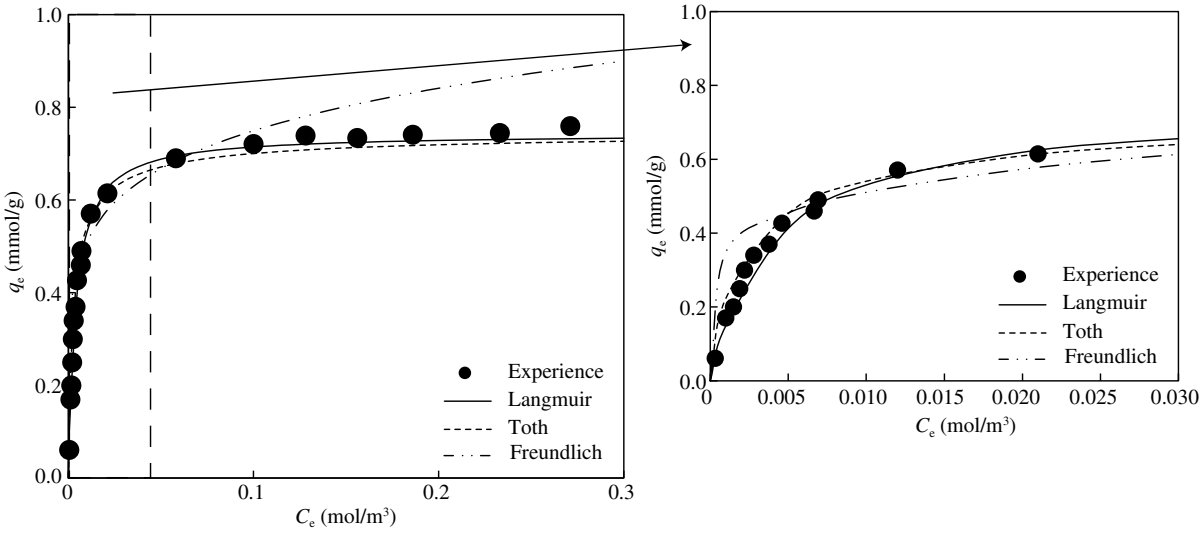

Fig. 2 – Adsorption isotherm of toluene on zeolite ZSM-5 at 300 K. C_e: toluene concentration at equilibrium; q_e: adsorbed quantity of toluene per mass of zeolite.

CVD80 (Agnihotri et al., 2005). A more detailed comparison with the adsorption capacities of other volatile organic compounds and zeolites reported in the literature is not helpful. Adsorption capacities are dependent on the Si/Al ratio. Channel intersections (four per cell) have been claimed as preferential adsorption sites for cyclic hydrocarbons (Song et al., 2007). Toluene adsorption could be due to strong interactions between the methyl group of the toluene molecule and acidic surface groups of ZSM-5 zeolite. Similar adsorption mechanism has been proposed for toluene adsorption onto MCM-41, NaY and SiO_2 (Zhang et al., 2012).

2.2. Toluene removal by the adsorption–ozonation process

The treatment of a simulated polluted air with toluene vapours was carried out at bench scale by a sequential process: adsorption followed by ozonation. The typical course of an experiment is represented in Fig. 3 for one cycle of adsorption–ozonation of toluene at room temperature.

Fig. 3a shows the evolution of the ratio of the concentration of toluene at the outlet and inlet of the reactor (C_{out}/C_{in}) as a function of time, during the adsorption step at 300 K (using 150 g of ZSM-5, 50 ppmV or 0.205 g_{C7H8}/m^3, and 5 m^3/hr). Experimental results of the ozonation step are depicted in Fig. 3b, using 18 g_{O3}/m^3 and a flow rate of 0.25 m^3/hr. A classical breakthrough adsorption curve was observed. During the first 20 min of adsorption, toluene was not detected at the reactor outlet stream. Then, it started to increase progressively as a function of time, reaching a 30% of the saturation value (C_{out}/C_{in} = 0.3) after around 120 min. The weak slope of the breakthrough dynamic adsorption curve of ZSM-5 can be explained by a wide mass transfer zone, probably limited by internal mass transfer resistances inside the zeolite pellets. When a 30% of the saturation was reached, 0.012 g_{C7H8}/g_{ZSM-5} is adsorbed (or 0.132 $mmol_{C7H8}/g_{ZSM-5}$), corresponding to 1.83 g of toluene for the whole zeolite bed. This value was in agreement with the static adsorption equilibrium value (Fig. 2, 0.3 $mmol_{C7H8}/g_{ZSM-5}$) and indicated that only 17.65% of the maximum adsorption capacity of the zeolite bed was used at this moment. After such condition, the inlet of polluted air was stopped and the ozonation of adsorbed toluene was carried out, switching the feeding to the O_3/air stream (18 g_{O3}/m^3 and 0.25 m^3/hr). A very high peak in the concentration of toluene at the reactor outlet stream was observed (Fig. 3b) as soon as the ozonation step began, indicating a high release of toluene by thermal desorption. During this phase, the temperature in the zeolite bed increased, reaching around 372 K. Such results were evidences that a fraction of the adsorbed toluene desorbed from the ZSM-5 surface due to local heating generated by toluene oxidation reactions with ozone.

After 60 min of ozonation the amount of desorbed toluene was about 5.34 × 10^{-3} $mmol/g_{ZSM-5}$, corresponding to 0.074 g

Table 2 – Langmuir, Freundlich and Toth parameters for toluene adsorption on ZSM-5 zeolite.

Langmuir parameters		Toth parameters		Freundlich parameters	
q_m (mol/kg)	0.75	q_m' (mol/kg)	0.79	k ($mol^{1-1/n}.m^{3-1/n}$/kg)	1.10
b (m^3/mol)	250	b' (($mol/m^3)^{t'}$)	987	n	7.5
		t'	0.71		
R^2	0.97	R^2	0.96	R^2	0.83

q_m: maximum adsorption capacity; b: adsorption equilibrium constant or Langmuir coefficient; q_m': maximum monolayer adsorption capacity parameter, b': Toth isotherm constant, t': dimensionless constant; k: adsorption equilibrium constant; and n: empirical constant of the Freundlich model.

Table 3 – Comparison of maximum adsorption capacities toward toluene of ZSM-5 and some other adsorbents reported in the literature.

Adsorbent	Temperature (K)	Maximum adsorption capacity		Reference
		(mmol/g)	($\times 10^3$ mmol/m^2)	
ZSM-5	298	0.93	3.01	Present work
NaZSM-5	473	0.92	2.5	Serra et al. (2012)
HMOR (Si/Al = 10)	473	1.07	2.2	Serra et al. (2012)
NaY	303	≈2.3	–	Jin and Zhu. (2000)
EA95	298	1.7	3.4	Agnihotri et al. (2005)
CVD80	298	1.6	2.6	Agnihotri et al. (2005)
MCM-41	298	4.98	3.3	Ma and Ruan (2013)
S-MCM	298	2.49	2	Ma and Ruan (2013)
MOF-177	298	6.06	2	Yang et al. (2013)
MCM-48	300.15	≈1.08–3.45	2.3–2.2	Shim et al. (2006)
Silica–alumina	300	0.085	0.13	Lee et al. (2008)
DAY zeolite	298	≈1.8	2.5	Lee et al. (2011)
	318	≈1.5	2.1	
Na-Y/H-Y/USY/ZSM-5	298	≈ 2–2.5 or 3–4	3.3–4.1	Takeuchi et al. (2012)

EA95 and CVD80 refer to single-wall carbon nanotubes manufactured by electric arc and the HiPco by chemical vapour deposition; DAY zeolite represents a dealuminated Y-zeolite.

of toluene for the whole bed, which accounted for 4.05% of the initially quantity of adsorbed toluene. It is important to note that in a normal industrial operation, the adsorption step would be stopped before the zeolite adsorption bed reached 30% of saturation. Under such condition, thermally desorbed VOCs could be trapped in the zeolite bed zone free of adsorbate or could be recycled.

When the first cycle of adsorption–oxidation finished, a new polluted air stream was sent again over the zeolite bed at the same conditions as been applied during the first adsorption step. As can be seen in Fig. 3, during the first 20 min of the second adsorption step, toluene was not detected. The breakthrough curve was quite the same, indicating that a regeneration of the zeolite bed had occurred.

2.3. Successive cycles of adsorption–ozonation treatments

Figs. 4, 5 and 6 depict the experimental results of four adsorption–oxidation (AD–OZ) cycles performed over the same zeolite sample, using the same operating conditions as described before. Fig. 4 displays the evolution of the ratio of the concentration of toluene at the outlet and inlet of the reactor during four consecutive adsorption–ozonation cycles, as a function of processed bed volumes of contaminated stream per mass of ZSM-5 zeolite.

As can be noticed in Fig. 4, during the four adsorption steps, breakthrough curves A, C, E, G, and I had the same appearances. In all cases, the adsorption time remained unchanged after the four consecutive adsorption–ozonation cycles (around 20 min, corresponding to a ratio of V_{gaz}/

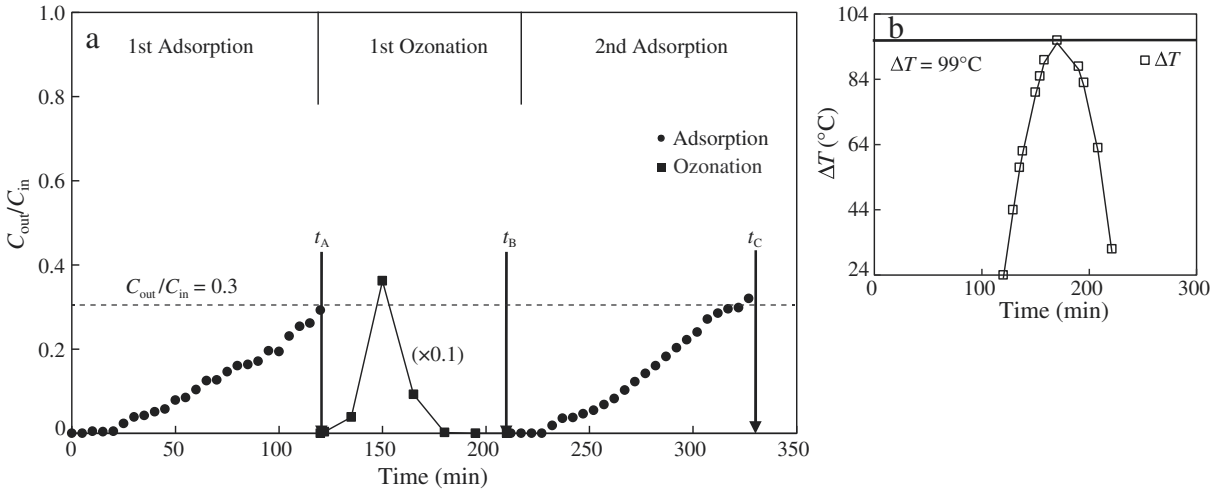

Fig. 3 – (a) Variation of the ratio of the concentration of toluene at the outlet and inlet (C_{out}/C_{in}) of the reactor with time and (b) temperature (T) variation of the ZSM-5 bed during the first cycle of the adsorption–ozonation treatment. Operating conditions: 150 g of ZSM-5, inlet flow of toluene 5 m^3/hr and 0.205 $g_{C_7H_8}$/m^3, and inlet flow of 18 g_{O_3}/m^3 ozone 0.25 m^3/hr.

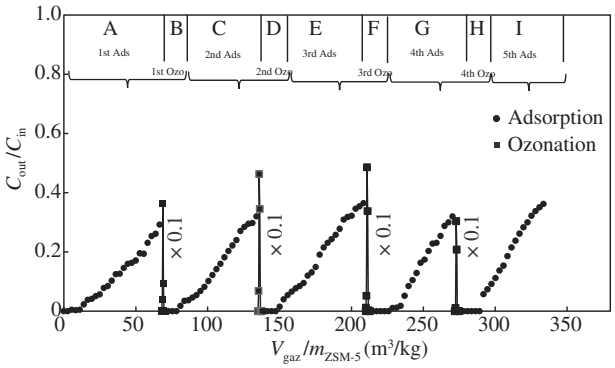

Fig. 4 – Evolution of the ratio of the concentration of toluene at the outlet and inlet of the reactor during four consecutive adsorption (AD)–ozonation (OZ) cycles using ZSM-5. Operating conditions: 150 g of ZSM-5, inlet flow of toluene 5 m^3/hr and 0.205 g_{C_7H8}/m^3, and inlet flow of 18 g_{O3}/m^3 ozone 0.25 m^3/hr.

kg_{ZSM-5} = 8.20 m^3/kg with C_{out}/C_{in} = 0). The comparison of the breakthrough time before and after the ozonation could be used as an estimate whether the adsorption capacity is recovered. Additionally, an increase in the concentration of toluene in the reactor outlet stream was also observed in Fig. 4, when the regeneration step using ozone was initiated (see curves B, D, F and H). These results were related to the registered increase of the temperature inside the reactor due to ozone reaction with adsorbed toluene, leading to a physical desorption of a fraction of the retained toluene.

Fig. 5 compares the results of five adsorption steps after different operating cycles of adsorption–ozonation. As can be seen, the adsorption breakthrough curves had the same appearance. The slopes had almost the same rate (3×10^{-3} min^{-1} for the 1st and 2nd cycle, 7×10^{-3} min^{-1} for the 3rd and 10^{-2} min^{-1} for the 4th cycle). Moreover, the same breakthrough time was found for each adsorption step, being around 57 min at C_{out}/C_{in} = 0.3. The results of the adsorption capacity recovery for each cycle are presented in Table 4 and

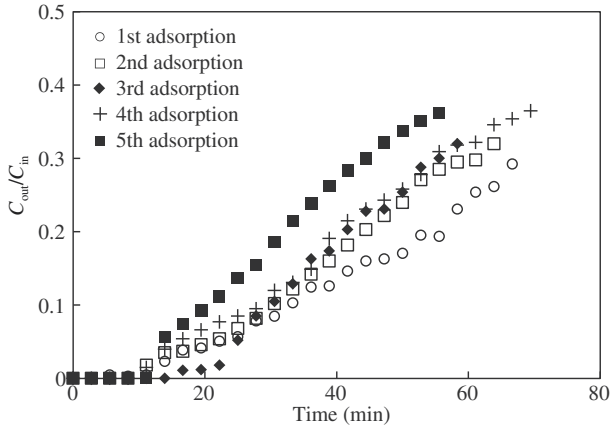

Fig. 5 – Comparison of toluene adsorption breakthrough curves after different cycles of adsorption–ozonation.

are determined using the following equation:

$$RE = \frac{Q^{A}_{cycle_{nc}}}{Q^{A}_{cycle_{1}}} \times 100\% \quad (9)$$

where, RE (%) stands for the adsorption capacity recovery, $Q^{A}_{cycle_1}$ (g_{C_7H8}/g_{ZSM-5}) represents the amount of adsorbed toluene in the first adsorption step and $Q^{A}_{cycle_{nc}}$ (g_{C_7H8}/g_{ZSM-5}) is the amount of adsorbed toluene in the specified cycle number (*nc*). The adsorption capacity recovery of ZSM-5 was very good (92%–99%). This high capacity recovery level is not only related to the regeneration of the sites, but also to the fact that adsorption sites are not totally saturated at the end of adsorption step. In addition, breakthrough time remained constant, and the amount of adsorbed toluene after each ozonation step was around 0.012 g_{C_7H8}/g_{ZSM-5}.

Table 4 also lists the values of toluene mineralisation factor (MIN). These observed mineralisation values were determined by taking into consideration the stoichiometric ratios in the gaseous reaction between toluene and ozone (see Eq. (10)) and using registered experimental results. Eq. (11) was applied in the estimation of process mineralisation capacity.

$$6O_3 + C_7H_8 \rightarrow 7CO_2 + 4H_2O \quad (10)$$

$$MIN = \frac{Q_{CO_2}}{Q^{A}_{C_7H_8}} \times \frac{1}{7} \times 100\% \quad (11)$$

where Q_{CO_2} (mol_{CO_2}/kg_{ZSM-5}) is the amount of CO_2 generated per mass of zeolite and $Q^{A}_{C_7H_8}$ (mol_{C_7H8}/kg_{ZSM-5}) is the adsorbed amount of toluene after the thermal desorption step. As is shown in Table 4, the process mineralisation capacity was very high, reaching values between 75% and 85%. These results could be related to the three-dimensional structure of zeolite framework with interconnected channels and the proximity between the pores, which allows surface interactions between toluene and ozone (Alejandro et al., 2014; Brodu et al., 2013). ZSM-5 could confine and increases the surface contact between ozone and toluene. Thus, in the presence of ZSM-5 zeolite, adsorbed toluene could be eliminated by a surface reaction mechanism that might include direct interaction with gaseous ozone and indirect reactions with surface radicals generated after ozone adsorption and decomposition at active surface sites of ZSM-5 zeolite.

Fig. 6 shows the evolution in the concentration of CO_2, ozone and toluene at the reactor outlet stream as a function of time during different cycles of AD–OZ treatments. Additionally, the temperature variation of ZSM-5 bed was also presented. During the ozonation steps, the profiles of the outlet concentration of ozone had a form of "S". The breakthrough time of ozone over the ZSM-5 bed was around 40 min for the four AD–OZ cycles. After that, the outlet concentration of ozone increased rapidly. At the end of the oxidation step, it was found that the outlet concentration of ozone tended to reach the inlet concentration as soon as the concentration of CO_2 decreased and became zero. A peak in the concentration of toluene was registered (3.6 to 4.6 times

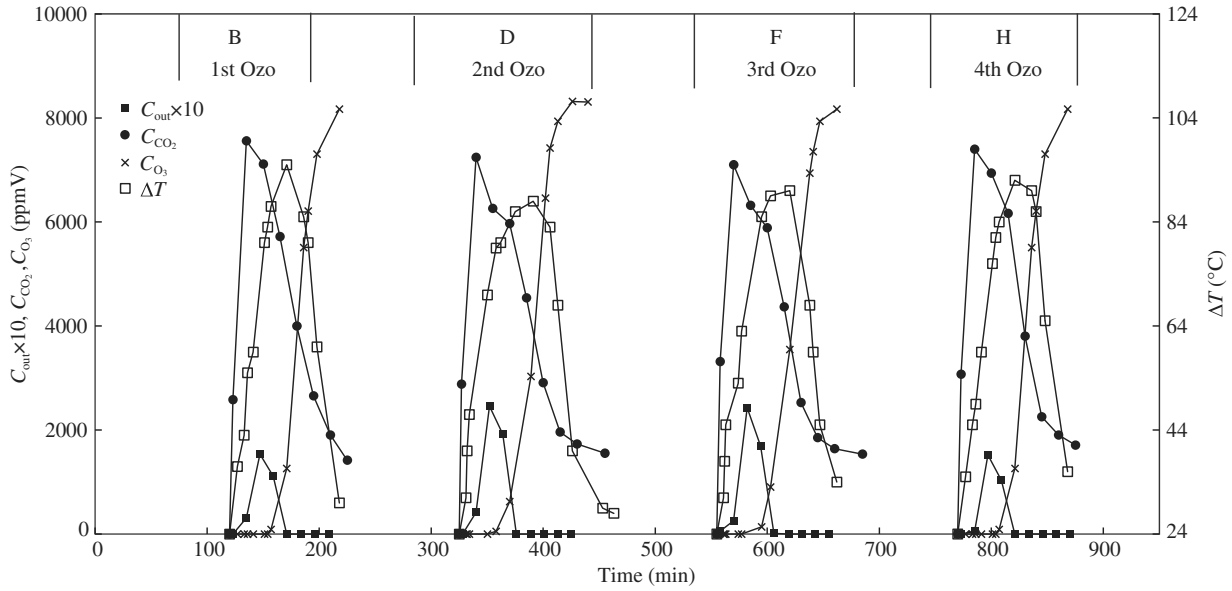

Fig. 6 – Variation of different operating parameters during four consecutive adsorption–ozonation cycles of toluene removal over ZSM-5. C_{out}: outlet concentration of toluene; C_{CO_2}: outlet concentration of CO_2; C_{O_3}: outlet concentration of ozone; ΔT: temperature variation of ZSM-bed.

the value of the initial concentration) at the beginning of the experiment. This result could be related to toluene desorption due to the increase on temperature during the oxidation reactions.

The number of mol of ozone consumed per mol of toluene oxidised (Y_{O_3/C_7H_8}) and the number of mol of CO_2 generated per mol of toluene oxidised (Y_{CO_2/C_7H_8}) are listed in Table 4. In the 1st cycle, a total amount of 0.133 $mol_{C_7H8}/kg_{ZSM\text{-}5}$ were adsorbed on ZSM-5 and only 0.005 $mol_{C_7H8}/kg_{ZSM\text{-}5}$ were desorbed. The amount of oxidised toluene was around 0.127 $mol_{C_7H8}/kg_{ZSM\text{-}5}$, which was about 97% of the total toluene removed in the AD–OZ system. Similar ratios (92%–93%) were obtained in the 2nd, 3rd and 4th cycles. In the 1st, 2nd, 3rd, and 4th AD–OZ cycles, 5.46, 6.12, 6.00 and 5.30 mol of ozone were consumed per mol of toluene oxidised, respectively, indicating that ozone was effectively used in toluene oxidation. These values were comparable to the stoichiometric ratio given by Eq. (10) (O_3/C_7H_8 = 6/1), showing that a significant amount of ozone was necessary for toluene oxidation. The amount of CO_2 generated per oxidised toluene during the AD–OZ treatment cycles was also investigated. Experimental ratios of 5.5/1, 5.9/1; 5.9/1 and 5.2/1 were found for the 1st, 2nd, 3rd and 4th cycles, respectively. These values were close to the stoichiometric ratio given by Eq. (10) (CO_2/

Table 4 – Mass balance of toluene ozonation over ZSM-5 zeolite.

Cycles	$Q^A_{C_7H_8}$ (mol/kg)	$Q^L_{O_3}$ (mol/kg)	$Q^D_{C_7H_8}$ (mol/kg)	Q_{CO_2} (mol/kg)	$Q^R_{O_3}$ (mol/kg)	$Q^R_{C_7H_8}$ (mol/kg)	RE (%)	MIN (%)	Y_{CO_2/C_7H_8} (mol/mol)	Y_{O_3/C_7H_8} (mol/mol)
1st cycle	0.133	1.083	0.005	0.700	0.694	0.127	–	79	5.5	5.468
2nd cycle	0.132	1.444	0.009	0.720	0.75	0.122	99	84	5.9	6.148
3rd cycle	0.128	1.111	0.010	0.702	0.708	0.118	96	85	5.9	6.003
4th cycle	0.132	1.028	0.006	0.662	0.667	0.126	99	75	5.2	5.291
5th cycle	0.123	–	–	–		–	93	–	–	–

Residence time and the inlet concentration of toluene were 0.16 sec and 0.205 g/m^3, respectively.
RE: the adsorption capacity recovery; MIN: mineralisation factor; Q_{CO_2}: the amount of CO_2 generated per mass of zeolite; $Q^A_{C_7H_8}$: the adsorbed amount of toluene per mass of zeolite; $Q^D_{C_7H_8}$: the total amount of desorbed toluene per mass of zeolite; $Q^L_{O_3}$: the total applied load of ozone per mass of zeolite; Y_{O_3/C_7H_8}: the number of moles of ozone consumed per mole of toluene oxidised, calculated by the equation $Y_{O_3/C_7H_8} = \frac{Q^R_{O_3}}{Q^R_{C_7H_8}}$; Y_{CO_2/C_7H_8}: the number of moles of CO_2 generated per mole of toluene oxidised, calculated by the equation $Y_{CO_2/C_7H_8} = \frac{Q_{CO_2}}{Q^R_{C_7H_8}}$; $Q^R_{O_3}$: the amount of ozone consumed per mass of zeolite, calculated by $Q^R_{O_3} = \frac{F\,C_{O_{3in}}}{m}\int_{t_A}^{t_B}(1-\frac{C_{O_{3out_T}}}{C_{O_{3in}}})dt$; $Q^R_{C_7H_8}$: the amount of oxidised toluene per mass of zeolite, calculated by $Q^R_{C_7H_8} = Q^A_{C_7H_8} - Q^D_{C_7H_8}$.

C_7H_8 = 7/1). The strong CO_2 production and ozone consumption were indicatives of toluene oxidation. Indeed, the formation of trace oxidation by-products such as acetic acid and acetaldehyde was also detected by GC–MS analysis. Their concentrations were much lower than toluene and CO_2. These intermediate by-products remained adsorbed on zeolite surface and they could be only indentified after methanol extraction. Such intermediate by-products were also detected by Brodu et al. (2012) after the ozonation of methyl ethyl ketone adsorbed on ZSM-5.

Three main mechanisms have been proposed to describe catalytic ozonation of VOCs (Oyama, 2000; Kasprzyk-Horden et al., 2003). One mechanism indicates that the adsorbed VOC (chemisorbed or physisorbed) could react directly with gaseous ozone (O_3) (after diffusion through the gas film to the zeolite surface). This type of interaction has been proposed for the catalytic ozonation of ethanol over SiO_2 (Kastner et al., 2005). Another mechanism suggests that ozone could be adsorbed on the catalyst surface and converted into radicals for subsequent VOC oxidation reactions (Jans and Hoigne, 1998). This reaction mechanism has been also used to describe the interaction of aqueous ozone and activated carbons during the oxidation of organic pollutants in waters during a kind of advanced oxidation process (Jans and Hoigné, 1998; Kasprzyk-Horden et al., 2003). Other research groups suggest that both the VOC and O_3 could be adsorbed on the catalyst surface, promoting a surface reaction between the two chemisorbed substrates, where O_3 decomposes catalytically into surface active oxygen species and subsequently reacts with the chemisorbed VOC (Roscoe and Abbatt, 2005; Chao et al., 2007; Brodu et al., 2013; Alejandro et al., 2014; Valdés et al., 2014). Hence, the fact that the observed number of mol of ozone consumed per mol of toluene oxidised was close to the theoretical stoichiometric ratio of O_3/C_7H_8 in the gaseous reaction (6/1), suggests that a surface interaction would mainly occur in the vicinity of the zeolite surface. Ozone in the gas phase could move down into the atmosphere close to the zeolite surface and reacts with adsorbed toluene molecules, leading to toluene oxidation.

3. Conclusions

In this research, a new process technology that combines adsorption followed by ozone oxidation was studied for controlling toluene emissions from industrial processes and indoor environments. Results obtained in this work showed that toluene adsorption onto ZSM-5 zeolite followed by ozone oxidation could be used as a hybrid process for the control of low levels of VOCs in gaseous streams. Experimental results indicated that the destructive efficiency of toluene vapours was greater than 95% at room temperature. The major oxidation by-products of toluene detected in this study were CO_2 and H_2O, and no significant secondary products were observed. After five cycles of AD–OZ treatment, there was no evidence of catalytic deactivation of ZSM-5. Hence, the AD–OZ process using ZSM-5 could be effectively applied as an alternative low cost treatment to destroy toxic organic pollutants from industrial emissions.

Acknowledgments

Authors gratefully acknowledge the Centre National pour la Recherche Scientifique et Technique of Morocco (CNRST) and the Centre National de la Recherche Scientifique of France (CNRS) with the Project (CNRST/CNRS Grant No. SPI 05/13), Comisión Nacional de Investigación Científica y Tecnológica (CONICYT) of Chile and Fondo Nacional de Desarrollo Científico y Tecnológico of Chile (FONDECYT) with the Project (CONICYT/FONDECYT Grant No. 1130560), Comité de Evaluation-orientation de la Coopération Scientifique of France (ECOS) and Comisión Nacional de Investigación Científica y Tecnológica of Chile (CONICYT), with the project (ECOS/CONICYT Grant No. C11E08), for their financial support.

REFERENCES

Agnihotri, S., Rood, M.J., Rostam-Abadi, M., 2005. Adsorption equilibrium of organic vapors on single-walled carbon nanotubes. Carbon 43 (11), 2379–2388.

Alejandro, S., Valdés, H., Manéro, M.-H., Zaror, C.A., 2014. Oxidative regeneration of toluene-saturated natural zeolite by gaseous ozone: the influence of zeolite chemical surface characteristics. J. Hazard. Mater. 274, 212–220.

Baek, S.W., Kim, J.R., Ihm, S.K., 2004. Design of dual functional adsorbent/catalyst system for the control of VOC's by using metal-loaded hydrophobic Y-zeolites. Catal. Today 93–95, 575–581.

Blocki, S.W., 1993. Hydrophobic zeolite adsorbent: a proven advancement in solvent separation technology. Environ. Prog. 12 (3), 226–230.

Bonjour, J., Chalfen, J.B., Meunier, F., 2002. Temperature swing adsorption process with indirect cooling and heating. Ind. Eng. Chem. Res. 41 (23), 5802–5811.

Brodu, N., Zaitan, H., Manero, M.H., Pic, J.S., 2012. Removal of volatile organic compounds by heterogeneous ozonation on microporous synthetic alumina silicate. Water Sci. Technol. 66 (9), 2020–2026.

Brodu, N., Manero, M.-H., Andriantsiferana, C., Pic, J.S., Valdés, H., 2013. Role of Lewis acid sites of ZSM-5 zeolite on gaseous ozone abatement. Chem. Eng. J. 231, 281–286.

Brosillon, S., Manero, M.H., Foussard, J.N., 2001. Mass transfer in VOC adsorption on zeolite: experimental and theoretical breakthrough curves. Environ. Sci. Technol. 35 (17), 3571–3575.

Chao, C.Y.H., Kwong, C.W., Hui, K.S., 2007. Potential use of a combined ozone and zeolite system for gaseous toluene elimination. J. Hazard. Mater. 143 (1-2), 118–127.

Cosseron, A.F., Daou, T.J., Tzanis, L., Nouali, H., Deroche, I., Coasne, B., et al., 2013. Adsorption of volatile organic compounds in pure silica CHA, ⁄BEA, MFI and STT-type zeolites. Microporous Mesoporous Mater. 173, 147–154.

Einaga, H., Teraoka, Y., Ogata, A., 2011. Benzene oxidation with ozone over manganese oxide supported on zeolite catalysts. Catal. Today 164 (1), 571–574.

Foster, K.L., Fuerman, R.G., Economy, J., Larson, S.M., Rood, M.J., 1992. Adsorption characteristics of trace volatile organic compounds in gas streams onto activated carbon fibers. Chem. Mater. 4 (5), 1068–1073.

Freundlich, H.M.F., 1906. Over the adsorption in solution. J. Phys. Chem. 57, 385–471.

Ghoshal, A.K., Manjare, S.D., 2002. Selection of appropriate adsorption technique for recovery of VOCs: an analysis. J. Loss Prev. Process Ind. 15 (6), 413–421.

Jans, U., Hoigné, J., 1998. Activated carbon and carbon black catalyzed transformation of aqueous ozone into OH-radicals. Ozone Sci. Eng. 20 (1), 67–90.
Jin, W., Zhu, S., 2000. Study of adsorption equilibrium and dynamics of benzene, toluene, and xylene on zeolite NaY. Chem. Eng. Technol. 23 (2), 151–156.
Kasprzyk-Horden, B., Ziólek, M., Nawrocki, J., 2003. Catalytic ozonation and methods of enhancing molecular ozone reactions in water treatment. Appl. Catal. B Environ. 46 (4), 639–669.
Kastner, J.R., Buquoi, Q., Ganagavaram, R., Das, K.C., 2005. Catalytic ozonation of gaseous reduced sulfur compounds using wood fly ash. Environ. Sci. Technol. 39 (6), 1835–1842.
Khan, F.I., Ghoshal, A.K., 2000. Removal of volatile organic compounds from polluted air. J. Loss Prev. Process Ind. 13 (6), 527–545.
Kwong, C.W., Chao, C.Y.H., Hui, K.S., Wan, M.P., 2008. Catalytic ozonation of toluene using zeolite and MCM-41 materials. Environ. Sci. Technol. 42 (22), 8504–8509.
Langmuir, I., 1916. The constitution and fundamental properties of solids and liquids. Part I. Solids. J. Am. Chem. Soc. 38 (11), 2221–2295.
Le Cloirec, P., 1998. Les Composés Organiques Volatils (COV) Dans l'environnement. TEC & DOC, Paris.
Lee, C.K., Chaing, A.S.T., 1996. Adsorption of aromatic compounds in large MFI zeolite crystals. J. Chem. Soc. Faraday Trans. 92 (18), 3445–3451.
Lee, S.W., Park, H.J., Lee, S.H., Lee, M.G., 2008. Comparison of adsorption characteristics according to polarity difference of acetone vapor and toluene vapor on silica–alumina fixed-bed reactor. J. Ind. Eng. Chem. 14 (1), 10–17.
Lee, D.G., Kim, J.H., Lee, C.H., 2011. Adsorption and thermal regeneration of acetone and toluene vapors in dealuminated Y-zeolite bed. Sep. Purif. Technol. 77 (3), 312–324.
Li, J.W., Pan, K.L., Yu, S.J., Yan, S.Y., Chang, M.B., 2014. Removal of formaldehyde over $Mn_xCe_{1-x}O_2$ catalysts: Thermal catalytic oxidation versus ozone catalytic oxidation. J. Environ. Sci. 26 (12), 2546–2553.
Ma, C.M., Ruan, R.T., 2013. Adsorption of toluene on mesoporous materials from waste solar panel as silica source. Appl. Clay Sci. 80–81, 196–201.
Meininghaus, C.K.W., Prins, R., 2000. Sorption of volatile organic compounds on hydrophobic zeolites. Microporous Mesoporous Mater. 35–36, 349–365.
Monneyron, P., Mathé, S., Manero, M.H., Foussard, J.N., 2003. Regeneration of high silica zeolites via advanced oxidation processes—a preliminary study about adsorbent reactivity toward ozone. Chem. Eng. Res. Des. 81 (9), 1193–1198.
Monneyron, P., Manero, M.H., Mathe, S., 2007. A combined selective adsorption and ozonation process for VOCS removal from air. Can. J. Chem. Eng. 85 (3), 326–332.
Oyama, T.S., 2000. Chemical and catalytic properties of ozone. Catal. Rev. Sci. Eng. 42 (3), 279–322.
Paints Directive 2004/42/EC, 2004. Directive 2004/42/CE of the European Parliament and of the Council of 21 April 2004 on the Limitation of Emissions of Volatile Organic Compounds Due to the Use of Organic Solvents in Certain Paints and Varnishes and Vehicle Refinishing Products Amending Directive 1999/13/EC. European Union Publications Office. (Retrieved on 2013-02-25).
Rafson, J.H., 1998. Odor and VOC Control Handbook. McGraw Hill, New York, NY.
Roscoe, J.M., Abbatt, J.P.D., 2005. Diffuse reflectance FTIR study of the interaction of alumina surfaces with ozone and water vapour. J. Phys. Chem. A 109 (40), 9028–9034.
Ruddy, E.N., Carroll, L.A., 1993. Select the best VOC control strategy. Chem. Eng. Prog. 89 (7), 28–35.
Serra, R.M., Miró, E.E., Bolcatto, P., Boix, A.V., 2012. Experimental and theoretical studies about the adsorption of toluene on ZSM5 and mordenite zeolites modified with Cs. Microporous Mesoporous Mater. 147 (1), 17–29.
Shim, W.G., Lee, J.W., Moon, H., 2006. Adsorption equilibrium and column dynamics of VOCs on MCM-48 depending on pelletizing pressure. Microporous Mesoporous Mater. 88 (1-3), 112–125.
Song, L.J., Rees, L.V.C., 2000. Adsorption and diffusion of cyclic hydrocarbon in MFI-type zeolites studied by gravimetric and frequency–response technique. Microporous Mesoporous Mater. 35–36, 301–314.
Song, L.J., Sun, Z.L., Duan, L.H., Gui, J.Z., McDougall, G.S., 2007. Adsorption and diffusion properties of hydrocarbons in zeolites. Microporous Mesoporous Mater. 104 (1-3), 115–128.
Takeuchi, M., Hidaka, M., Anpo, M., 2012. Efficient removal of toluene and benzene in gas phase by the TiO_2/Y-zeolite hybrid photocatalyst. J. Hazard. Mater. 237-238, 133–139.
Toth, J., 1971. State equations of the solid gas interface layer. Acta Chem. Acad. Hung. 69, 311–317.
Valdés, H., Solar, V.A., Cabrera, E.H., Veloso, A.F., Zaror, C.A., 2014. Control of released volatile organic compounds from industrial facilities using natural and acid-treated mordenites: the role of acidic surface sites on the adsorption mechanism. Chem. Eng. J. 244, 117–127.
Vinh-Thang, H., Huang, Q.L., Eic, M., Trong-On, D., Kaliaguine, S., 2005. Adsorption of C-7 hydrocarbons on biporous SBA-15 mesoporous silica. Langmuir 21 (11), 5094–5101.
VOC Solvents Directive 1999/13/EC, 1999. Council Directive 1999/13/EC of 11 March 1999 on the Limitation of Emissions of Volatile Organic Compounds Due to the Use of Organic Solvents in Certain Activities and Installations. European Union Publications Office (Retrieved on 2013-02-25).
Yang, R.T., 1987. Gas Separation by Adsorption Processes. Butterworths, Boston.
Yang, K., Xue, F., Sun, Q., Yue, R.L., Lin, D.H., 2013. Adsorption of volatile organic compounds by metal-organic frameworks MOF-177. J. Environ. Chem. Eng. 1 (4), 713–718.
Yu, F.D., Luo, L.G., Grevillot, G., 2007. Electrothermal swing adsorption of toluene on an activated carbon monolith: experiments and parametric theoretical study. Chem. Eng. Proces. 46 (1), 70–81.
Zaitan, H., Korrir, A., Chafik, T., Bianchi, D., 2013. Evaluation of the potential of volatile organic compound (*di-methyl benzene*) removal using adsorption on natural minerals compared to commercial oxides. J. Hazard. Mater. 262, 365–376.
Zhang, W.W., Qu, Z.P., Li, X.Y., Wang, Y., Ma, D., Wu, J.J., 2012. Comparison of dynamic adsorption/desorption characteristics of toluene on different porous materials. J. Environ. Sci. 24 (3), 520–528.